NACA

RESEARCH MEMORANDUM

A THEORETICAL ANALYSIS OF A SIMPLE AERODYNAMIC DEVICE TO IMPROVE THE LONGITUDINAL DAMPING OF A CRUCIFORM MISSILE CONFIGURATION AT SUPERSONIC SPEEDS

By James E. Clements

Langley Aeronautical Laboratory
Langley Field, Va.

NATIONAL ADVISORY COMMITTEE
FOR AERONAUTICS

WASHINGTON
October 27, 1955

Classification cancelled (or changed to Unclassified)

By Authority of Ltr to P.S. Announcement #19
(OFFICER AUTHORIZED TO CHANGE)

By ..... 29 May 57

.....
(GRADE OF OFFICER MAKING CHANGE)

31 May 57
DATE

NATIONAL ADVISORY COMMITTEE FOR AERONAUTICS

RESEARCH MEMORANDUM

A THEORETICAL ANALYSIS OF A SIMPLE AERODYNAMIC DEVICE TO IMPROVE THE LONGITUDINAL DAMPING OF A CRUCIFORM MISSILE CONFIGURATION AT SUPERSONIC SPEEDS

By James E. Clements

SUMMARY

A theoretical analysis of a cruciform missile configuration equipped with floating controls has been performed to determine if such controls can be utilized to improve the airframe transient response characteristics. This investigation covers either forward or aft locations of the floating controls at supersonic speeds. The analytical investigation was conducted mainly by factoring the characteristic equation of the system and examining the roots of the airframe and control modes of motion although other supplementary techniques were employed.

The results of this investigation indicate that, for operation of the floating-control airframe over the Mach number and altitude ranges considered in this analysis, a substantial increase in airframe damping can be obtained through a proper selection of the hinge-moment coefficients and through the use of a fixed-rate viscous damper attached to the floating-control surfaces.

A method is presented in the appendix to predict the maximum airframe damping and the associated control-surface damping rate for any prescribed values of the hinge-moment coefficients at any flight condition.

INTRODUCTION

As part of the research program concerned with simplifying missile control systems, the Automatic Control Dynamics Section of the Langley Pilotless Aircraft Research Division has conducted investigations on some simple aerodynamic devices to augment missile damping. This paper investigates the effect of viscously restrained free-floating controls (henceforth referred to as floating controls) on the damping in pitch of a cruciform canard finned missile in supersonic flight. The increase in

missile damping results from the introduction of a control damper to supply the necessary phase lag between the airframe and control motion in combination with a proper selection of the hinge-moment coefficients. The control surfaces are free to float to their equilibrium position restrained only by the viscous damper. Furthermore, the control-surface damping rate is assumed to result entirely from the viscous damper (aerodynamic contribution is considered negligible). The results are presented in the form of stability plots and damping plots for various control characteristics and flight conditions.

Similar studies along these lines have been conducted for airplanes with free-floating control surfaces. A theoretical analysis is presented in reference 1 and the results of a flight test are given in reference 2.

SYMBOLS

m	airframe mass, 5.05 slugs
$\bar{c}$	wing mean aerodynamic chord, 1.776 ft
$\bar{c}_c$	floating-control mean aerodynamic chord, 0.458 ft
S	total wing area, one plane, 4.1 sq ft
S_c	floating-control exposed area, one plane, 0.281 sq ft
I_Y	moment of inertia of airframe about Y-axis, 31.3 slug-ft^2
I_c	moment of inertia of floating control about hinge line, 0.00244 slug-ft^2
V	velocity, ft/sec
q	dynamic pressure, lb/sq ft
l_h	distance between airframe center of gravity and floating-control hinge line, ft
θ	pitch angle, radians
α	angle of attack, radians
δ	floating-control-surface deflection angle, radians
M	Mach number

$T_{1/2}$ time to damp to half amplitude

C_L lift coefficient, $\frac{\text{Lift}}{qS}$

C_m pitching-moment coefficient, $\frac{\text{Pitching moment}}{qS\bar{c}}$

C_h hinge-moment coefficient, $\frac{H}{qS_c\bar{c}_c}$

$$C_{L_\alpha} = \frac{\partial C_L}{\partial \alpha}$$

$$C_{L_\delta} = \frac{\partial C_L}{\partial \delta}$$

$$C_{m_\alpha} = \frac{\partial C_m}{\partial \alpha}$$

$$C_{m_\delta} = \frac{\partial C_m}{\partial \delta}$$

$$C_{m_q} = \frac{\partial C_m}{\partial \dot{\theta} \frac{\bar{c}}{2V}}$$

$$C_{m_{\dot{\alpha}}} = \frac{\partial C_m}{\partial \dot{\alpha} \frac{\bar{c}}{2V}}$$

$$C_{h_\alpha} = \frac{\partial C_h}{\partial \alpha}$$

$$C_{h_\delta} = \frac{\partial C_h}{\partial \delta}$$

$$C_{h_{\dot{\delta}}} = \frac{\partial C_h}{\partial \dot{\delta}}$$

$$C_{h_{\dot{\theta}}} = \frac{\partial C_h}{\partial \dot{\theta}}$$

H hinge moment, ft-lb

$H_{\dot{\delta}} = \frac{\partial H}{\partial \dot{\delta}}$

ζ_a airframe percent critical damping parameter

ζ_c floating-control percent critical damping parameter

ω_{n_a} airframe undamped natural frequency, radians per second

ω_{n_c} floating-control undamped natural frequency, radians per second

p differential operator, d/dt

A,B,C,D,E coefficients of fourth-order characteristic equations

ζ_a', ζ_c', ω_{n_a}', ω_{n_c}' values of ζ_a, ζ_c, ω_{n_a}, and ω_{n_c} at peak airframe damping

DESCRIPTION OF AIRFRAME AND APPARATUS

The airframe utilized in this analysis is a cruciform canard finned missile. The wings and canards have leading edges swept back 60° and are in line. Listed in table I are the estimated stability derivatives for a static margin of 56 percent mean aerodynamic chord at $M = 1.6$, over a Mach number range. Additional stability derivatives for other values of static margin can be obtained from reference 3. A sketch of the model is presented in figure 1 along with the basic mass and dimensional characteristics.

The canards and wing-tip controls are of delta plan form with approximately equal lever arms to the airframe center of gravity. Throughout the analysis it is assumed that the floating-control surfaces are mass balanced and the hinge-moment coefficients C_{h_α} and C_{h_δ} can be readily obtained for the delta plan form through a selection of the hinge-line location and if necessary the addition of springs. A further assumption to simplify the analytical computation is that the inertia about the hinge line of the wing-tip control surface and the canard surface is the same.

Presented in figure 2 is a sketch of a proposed viscous damper that was built and bench tested to determine if the values of the floating-control-surface damping rates covered in this investigation were realizable.

Also shown in figure 2 is a typical installation for either floating canards or wing-tip controls.

The results of the bench test indicate that damping rates between 0.5 and 3.0 ft-lb/radian/sec can be obtained from this type of damper using silicone base fluids with viscosities between 50,000 and 1,000,000 centistokes. A possible disadvantage to this type of damper was also disclosed in the bench test. At low hinge moments, the damping rate tended to increase due to friction in the "O" ring seals and bearings. Furthermore, at low hinge moments the damping fluid no longer has the tendency to shear but becomes more elastic in nature and resistant to shear. The effect of this nonlinear damping action on the dynamic characteristic of a missile configuration in flight is not known but is not felt to be serious because of the large aerodynamic unbalanced controls utilized in this investigation.

METHODS OF ANALYSIS

Equations of Motion

The airframe equations of motion in pitch, assuming two degrees of freedom with constant forward velocity, are linear differential equations with constant coefficients and are as follows:

$$\frac{mV}{qS}(\dot{\theta} - \dot{\alpha}) = C_{L_\alpha}\alpha + C_{L_\delta}\delta \tag{1}$$

$$\frac{I_Y}{qS\bar{c}}\ddot{\theta} = C_{m_\alpha}\alpha + C_{m_\delta}\delta + C_{m_q}\frac{\bar{c}}{2V}\dot{\theta} + C_{m_{\dot{\alpha}}}\frac{\bar{c}}{2V}\dot{\alpha} \tag{2}$$

The differential equation describing the motion of the floating controls is

$$\frac{I_c}{qS_c\bar{c}_c}(\ddot{\theta} + \ddot{\delta}) = C_{h_\alpha}\alpha + C_{h_\delta}\delta + C_{h_{\dot{\delta}}}\dot{\delta} + C_{h_{\dot{\theta}}}\dot{\theta} \tag{3}$$

where the floating controls are assumed mass balanced and with the substitution:

$$C_{h_{\dot{\theta}}} = C_{h_\alpha}\left(\frac{l_h}{V}\right) \quad \text{for controls aft of center of gravity}$$

$$C_{h_{\dot{\theta}}} = C_{h_\alpha}\left(-\frac{l_h}{V}\right) \quad \text{for controls forward of center of gravity.}$$

The effect of the upwash created by the vortices shed from the forward control surfaces on the floating wing-tip controls was initially considered and was found to have a negligible effect on the airframe dynamics and therefore is not included in this analysis.

Combining the airframe equations of motion and the floating-control equation and solving for the characteristic equation of the system results in a fourth-degree polynominal of the form

$$Ap^4 + Bp^3 + Cp^2 + Dp + E = 0 \tag{4}$$

where the variable p is the differential operator d/dt.

Defining the coefficients of the characteristic equations as variables in C_{h_α}, C_{h_δ}, and $C_{h_{\dot{\delta}}}$ gives

$$A = a_1 b_1 c_1$$

$$B = a_2 b_1 c_1 - a_1 b_2 c_1 - a_1 b_4 c_1 - a_1 b_1 C_{h_{\dot{\delta}}}$$

$$C = a_1 b_5 c_1 - a_1 b_3 c_1 - a_3 b_4 c_1 - a_2 b_2 c_1 + a_1 b_4 C_{h_{\dot{\delta}}} - a_2 b_1 C_{h_{\dot{\delta}}} + a_1 b_2 C_{h_{\dot{\delta}}} - a_1 b_1 C_{h_\delta}$$

$$D = a_2 b_5 c_1 - a_3 b_3 c_1 + a_1 b_3 C_{h_{\dot{\delta}}} + a_2 b_2 C_{h_{\dot{\delta}}} + a_1 b_4 C_{h_\delta} + a_1 b_2 C_{h_\delta} - a_2 b_1 C_{h_\delta} + a_3 b_1 C_{h_\alpha} - a_1 b_5 c_2 C_{h_\alpha} + a_3 b_4 c_2 C_{h_\alpha}$$

$$E = a_1 b_3 C_{h_\delta} + a_2 b_2 C_{h_\delta} + a_3 b_3 c_2 C_{h_\alpha} - a_3 b_2 C_{h_\alpha} - a_2 b_5 c_2 C_{h_\alpha} - a_1 b_5 C_{h_\alpha}$$

where

$$a_1 = \frac{mV}{qS} \qquad a_2 = C_{L_\alpha} \qquad a_3 = C_{L_\delta}$$

$$b_1 = \frac{I_Y}{qS\bar{c}} \qquad b_2 = C_{m_q} \frac{\bar{c}}{2V} \qquad b_3 = C_{m_\alpha} \qquad b_4 = C_{m_{\dot{\alpha}}} \frac{\bar{c}}{2V} \qquad b_5 = C_{m_\delta}$$

$$c_1 = \frac{I_c}{qS_c c_{\bar{c}}} \qquad c_2 = \frac{l_h}{V}$$

Stability Criterion

The Routh-Hurwitz stability criterion was utilized to construct stability boundary plots for the floating-control airframe. The Routh criterion simply states that for a fourth-degree polynominal, if all powers are present and have the same algebraic sign, then for stability the following relation must be satisfied:

$$(BC - AD)D - B^2E > 0$$

Solving the Hurwitz determinant for a fourth-degree polynominal yields the following conditions for stability:

$$A > 0$$

$$B > 0$$

$$E > 0$$

$$(BC - AD) > 0$$

$$(BC - AD)D - B^2E > 0$$

which is precisely Routh's criterion; for, if all the coefficients are positive, then the only independent equation is the last. A more complete presentation of the Routh-Hurwitz stability criterion can be found in reference 4.

For this analysis, the airframe neutral oscillatory-stability boundary is determined by letting $(BC - AD)D - B^2E = 0$ and the floating-control static-stability boundary defined by letting $E = 0$. In each case the coefficients of the characteristic equation are written as variables in C_{h_α}, C_{h_δ}, and $C_{h_{\dot{\delta}}}$.

Analysis of the Airframe and Control Dynamic Characteristics

One approach to this type of investigation is to plot lines of constant $T_{1/2}$ (time to damp to half amplitude) for the airframe in the stable region. Examples of an application of this technique for a fourth-degree characteristic equation can be found in reference 5. Although this type of analysis was valuable in establishing the region of improved airframe damping, little information as to the dynamic characteristics of the airframe was obtained in spite of the lengthy machine computation necessary to compute a family of constant $T_{1/2}$ curves. The method adopted consisted of factoring the characteristic equation of the system in order

to observe the effect on ζ and ω_n of varying the control characteristics. In this way the dynamic characteristics of the missile can be expressed in a quadratic form as is usual in many applications. It should be remembered when analyzing the results that in most cases an increase in the airframe percent critical damping parameter ζ is usually accompanied by a decrease in the airframe undamped natural frequency ω_n, so that it is possible to actually increase $T_{1/2}$ even though ζ may increase.

Defining the coefficients of the characteristic equation as variables in terms of the hinge-moment coefficients and factoring over a range of the coefficients results in two quadratic expressions representing the airframe and control modes of motion. In general, the airframe mode is composed of two complex conjugate roots and the control mode is composed of either two complex conjugate or two real roots depending upon the magnitude of control damping. The advantage in factoring the characteristic equation is readily apparent in that the trends of damping and natural frequency for both modes of motion can be observed as the hinge-moment coefficients are varied.

RESULTS AND DISCUSSION

The cruciform airframe of figure 1 has been analyzed with floating controls either aft or forward of the airframe center of gravity. The flight conditions investigated are $M = 1.2$, 1.6, and 2.0 at sea level and $M = 1.2$ at 15,000 feet.

Stability Boundaries

The stable region for the airframe with floating controls is shown in figure 3 as a plot of the floating-control parameters C_{h_α}, C_{h_δ}, and $C_{h_{\dot{\delta}}}$. The boundaries of the stable region are formed by the airframe oscillatory boundary and the control static-stability boundary. The airframe oscillatory boundary is determined by one of the roots of the stability condition $(BC - AD)D - B^2E = 0$. Crossing the airframe oscillatory boundary from the stable region yields for the airframe mode a pair of complex conjugate roots with positive real parts. The control static-stability boundary is determined by letting $E = 0$ and is invariant with control-surface damping. Crossing the control static-stability boundary from the stable region will result in a pair of real roots, one of which is positive for the control mode.

The region of improved airframe damping in the stable region is determined by factoring the characteristic equation. For floating controls forward, positive C_{h_α} is required to improve the airframe response and, conversely, with floating controls aft, negative C_{h_α} is required.

Omitted from figure 3 for clarity is the position of the airframe oscillatory boundary at values of control-surface damping approaching the magnitude of the available aerodynamic control-surface damping. At these low values of control-surface damping, the movement of the airframe oscillatory boundary with increasing increments of control-surface damping is opposite from that shown in figure 3 in that the stable region increases in size as $C_{h_{\dot{\delta}}}$ is increased until at a particular value of $C_{h_{\dot{\delta}}}$ it will again begin to decrease and exhibit the trend as shown in figure 3. Also, at these low values of control-surface damping, the sign of C_{h_α} to give improved airframe damping will be opposite from that necessary at the higher values of $C_{h_{\dot{\delta}}}$. Although it is possible at low values of $C_{h_{\dot{\delta}}}$ to improve the airframe damping, this region becomes of little value because of the very limited improvement in the airframe response that is possible. The remainder of this investigation will be concerned with the region of improved damping at the higher values of $C_{h_{\dot{\delta}}}$ where a very significant increase in airframe damping is attainable.

Airframe Dynamic Characteristics

To analyze the effect of varying the hinge-moment parameters C_{h_α}, C_{h_δ}, and $C_{h_{\dot{\delta}}}$ on the damping of the airframe, lines of constant $T_{1/2}$ were plotted and the characteristic equation was factored through a range of flight conditions and control characteristics. As both methods of analysis require extensive computation, machine calculation is necessary.

Constant $T_{1/2}$ plots.- In figure 4 a typical result of plotting lines of constant $T_{1/2}$ is presented. The data are for one value of control-surface damping $C_{h_{\dot{\delta}}}$ and for one flight condition. For the basic fixed-control airframe, the time to damp to half amplitude is 0.194 second for the flight conditions of figure 4. From figure 4 it is shown that under the specified conditions of the control parameters the time to damp to half amplitude can be reduced to 0.0578 second or by as much as 70 percent. Also from figure 4 it can be seen that for a value of $C_{h_\delta} = -0.2$ to -0.3 the greatest improvement in airframe response can be achieved at smaller magnitudes of C_{h_α}. From additional plots of this type for other values of control-surface damping and flight conditions, it can be established

that this value of C_{h_δ} remains essentially constant. This suggests that once this pseudo-optimum value of C_{h_δ} has been determined the analysis can be simplified through the elimination of C_{h_δ} as a variable. A plot of constant $T_{1/2}$ in the $C_{h_\alpha}, C_{h_{\dot{\delta}}}$ plane can then be constructed, presenting a more complete picture of the effect of varying C_{h_α} and $C_{h_{\dot{\delta}}}$ on the airframe response.

Effect on the airframe mode of varying the control parameters.- To understand more clearly how variations in the control parameters affect the airframe and control modes of motion, the characteristic equation was factored for a range of control parameters and the roots examined. A constant C_{h_δ} was assumed based upon the results of the constant $T_{1/2}$ analysis. Presented in figure 5 is the general trend of airframe damping and natural frequency as the control parameters C_{h_α} and $C_{h_{\dot{\delta}}}$ are varied along a constant C_{h_δ} line in the stable region as shown in the inset. The origin of the curves represents the damping and natural frequency of the airframe when C_{h_α} equals zero or approximately the damping and natural frequency of the fixed-control airframe. In figure 5 an additional characteristic of floating controls is shown. At low values of $C_{h_{\dot{\delta}}}$ the natural frequency of the airframe can be appreciably changed without materially affecting the damping of the airframe. Although magnitudes are not shown in figure 5, the change in natural frequency can be as much as double or half the original frequency. This effect on ω_{n_a} at low $C_{h_{\dot{\delta}}}$ is easily calculated since, depending on the floating tendency, the control simply adds or subtracts to the static-stability parameter as follows:

$$\Delta C_{m_\alpha} = - \frac{C_{h_\alpha}}{C_{h_\delta}} C_{m_\delta}$$

The useful region for this investigation is the upper left portion of figure 5 where improved airframe damping is obtained as a result of adding damping to the floating control through a viscous damper. The effect of adding damping to the floating control is to cause the control motion to lag the airframe displacement and to become more in phase with the rate of displacement thereby providing increased airframe damping.

Effect of viscous damper on airframe dynamics.- In figure 6 this region of improved airframe damping is plotted for the floating-controls-aft case at $M = 1.2$, 1.6, and 2.0 at sea level and $M = 1.2$ at 15,000 feet. It can be seen from an examination of these plots that no

one value of $C_{h_{\dot{\delta}}}$ can be selected that would give the maximum improvement in airframe damping for any value of C_{h_α} or any Mach number but that a compromised value of $C_{h_{\dot{\delta}}}$ could probably be selected that could very nearly give the maximum improvement possible. For example, from figure 6, maintaining a value of $C_{h_{\dot{\delta}}} = -0.004$ as the Mach number varies from 1.2 to 2.0 at constant altitude would almost give the maximum improvement in airframe damping for any operating value of C_{h_α} through this Mach number range. As the dynamic pressure will increase by approximately a factor of 2 through this Mach number range, maintaining a constant $C_{h_{\dot{\delta}}}$ would probably present a rather complex mechanical problem in that the damping rate $\left(H_{\dot{\delta}}\right)$ of the viscous damper would have to decrease by a factor of 2 in order for $C_{h_{\dot{\delta}}}$ to remain constant. Assuming that this would be an unnecessary additional complexity, a more feasible approach from the viewpoint of simplifying the viscous damper would be to design the damper for one average damping rate through the expected Mach number range.

When altitude variation for the floating-control airframe is considered, a more favorable situation exists because the value of $C_{h_{\dot{\delta}}}$ that gives maximum improvement in airframe damping at a particular value of C_{h_α} will increase as the altitude increases. This can be seen by comparing the plots for $M = 1.2$ at sea level and 15,000 feet in figure 6. The increase in the optimum value of $C_{h_{\dot{\delta}}}$ will tend to offset the decrease in dynamic pressure thereby maintaining a fairly constant design damping rate $H_{\dot{\delta}}$ to give maximum improvement in airframe damping as the altitude varies.

If the viscous damper is to be designed for one damping rate as the Mach number varies, some value of airframe damping other than the maximum possible at a particular value of C_{h_α} will result. Figure 7 shows how $C_{h_{\dot{\delta}}}$ will vary with Mach number if a constant damping rate is assumed. The shaded area is plotted from the data of figure 6, and represents the range of $C_{h_{\dot{\delta}}}$ that gives maximum airframe damping for values of C_{h_α} between -0.5 and -0.9. The two values of $H_{\dot{\delta}}$ were chosen to give nearly maximum airframe damping characteristics at $M = 1.2$ and 1.6.

For either of the two values of $H_{\dot{\delta}}$ selected, some value of airframe damping other than the maximum possible will result. This is demonstrated in figure 8 where the airframe damping has been plotted against Mach number for the two constant values of $H_{\dot{\delta}}$. The dashed curve represents the maximum damping possible as taken from figure 6 and the solid curve is the airframe damping that results when a constant $H_{\dot{\delta}}$ is assumed.

The shaded area then represents the penalty in airframe damping due to using a constant $H_{\dot{\delta}}$ for the two values of C_{h_α} shown. It can be seen from figure 8 that for values of C_{h_α} equal to or greater than -0.5 either of the two values of $H_{\dot{\delta}}$ allows a minimum improvement in airframe damping of greater than a factor of two.

From the results of figure 8 and knowing that the optimum value of $C_{h_{\dot{\delta}}}$ increases with increasing altitude as previously discussed, it appears that a viscous damper could be designed for one damping rate that would give an appreciable improvement in the airframe damping over the Mach number and altitude ranges covered in this investigation.

Relation Between Airframe and Control Modes

The airframe dynamic characteristics are given as functions of the control dynamic characteristics in figures 9 and 10. Figure 9 shows that the peak airframe damping for any value of C_{h_α} occurs at a constant value of the control damping parameter ζ_c and is unique with each flight condition. In figure 10 it is also to be noted that the peak airframe damping for any value of C_{h_α} occurs at a constant ratio of the airframe and control undamped natural frequencies. The origin of the curves again represents the damping and natural frequency ratio of the floating-control airframe when C_{h_α} equals zero.

To determine if the trends of figures 9 and 10 were valid for some other value of C_{h_δ}, additional plots similar to figures 6, 9, and 10 were constructed for a value of $C_{h_\delta} = -0.5$. The results are presented in figure 11 for $M = 1.2$ at sea level. The trend of the maximum airframe damping always occurring at constant values of ζ_c and $\omega_{n_c}/\omega_{n_a}$ is still seen to be true.

Figures 9, 10, and 11 will be utilized more extensively in the appendix where a rapid method for predicting the viscous-damper requirements and the resulting airframe damping for any combination of C_{h_α} and C_{h_δ} is presented.

General Comments on the Application of Floating Controls

The hinge-moment characteristics of the half-delta control surfaces are such that if the hinge line is adjusted for the desired $C_{h_\alpha}, C_{h_\delta}$ relation it becomes possible for the control mode to be statically unstable at subsonic and near supersonic speeds. This is particularly true

for the controls-forward situation (positive C_{h_α} to improve missile damping) because the tendency is for C_{h_α} to increase positively as transonic flight is approached moving the control characteristic toward or into the unstable region. For a ground-launched missile with the floating controls forward, some means would have to be devised to lock the floating surfaces until supersonic flight is attained.

When selecting the control-surface damping rate, it should be remembered that it is generally possible to obtain the same value of airframe damping at two values of $C_{h_{\dot{\delta}}}$ (fig. 6). The lower value will in most cases cause an appreciable reduction in the airframe natural frequency resulting in little or no improvement in the time to damp to half amplitude for the airframe mode. If possible, the damping rate should be selected to give the smallest variation in airframe natural frequency over the expected Mach number and altitude ranges.

There are generally two methods used to adjust the hinge-moment characteristics. They are (1) the adjustment of the hinge-line position and (2) the addition of springs. These two methods are often used singularly or together depending on the desired ratio of C_{h_α} and C_{h_δ}. If springs are used to adjust C_{h_δ}, then it should be remembered that the value of C_{h_δ} will no longer remain constant with Mach number and altitude as assumed in the analysis but will be a direct function of dynamic pressure. Furthermore, if spring-restrained control surfaces are used, the ratio of control natural frequency to airframe natural frequency (fig. 10) will not be independent of altitude since C_{h_δ} is the sum of the aerodynamic and spring-restraint contributions. Extending this line of reasoning further, it is also possible for the spring-restrained floating-control airframe to be stable at one Mach number or altitude and become unstable at some other Mach number or altitude since the spring-restraint contribution to C_{h_δ} can either add or subtract depending upon dynamic pressure.

CONCLUDING REMARKS

From the results of this investigation, it can be concluded that a substantial improvement in airframe damping is possible utilizing floating controls. The data presented emphasize the importance of adjusting the floating-control hinge-moment coefficients and the need for a control-surface damper to provide artificial damping about the floating-control hinge line. Furthermore, if the floating-control damper is designed for only one damping rate, it is still possible to obtain a substantial

improvement in airframe damping over a limited Mach number range and altitude range.

In all cases investigated, an increase in airframe damping was accompanied by a decrease in the airframe natural frequency. This decrease in natural frequency can conceivably increase the airframe transient response time even though the percent critical damping parameter may increase. The reduction in airframe natural frequency can be minimized through a proper selection of the floating-control damping rate.

A method is presented in the appendix to estimate rapidly the maximum airframe percent critical damping and the floating-control damping rate for any combination of the floating-control hinge-moment coefficients C_{h_α} and C_{h_δ} and any flight condition.

Langley Aeronautical Laboratory,
National Advisory Committee for Aeronautics,
Langley Field, Va., August 24, 1955.

APPENDIX

METHOD FOR ESTIMATING AIRFRAME AND VISCOUS DAMPER CHARACTERISTICS

The two techniques employed in this investigation to analyze the floating-control airframe required lengthy machine computation. In an effort to shorten the computation time, a method is presented herein which allows the prediction of the floating-control airframe characteristics at the peak values of airframe damping for any combination of C_{h_α} and C_{h_δ}.

In order to predict the peak value of airframe damping ζ_a' and the associated floating-control dynamic characteristics ζ_c' and ω_{n_c}', the significant trends of figures 9, 10, and 11 will be utilized. First a method will be derived to predict the value of the ratio $\omega_{n_c}'/\omega_{n_a}'$ and the value of ζ_c' at the peak values of airframe damping as shown in figures 9, 10, and 11.

Determination of the Ratio $\omega_{n_c}/\omega_{n_a}$

From figures 10 and 11(c) it is seen that the value of the ratio $\omega_{n_c}/\omega_{n_a}$ at peak airframe damping is the same as the value of the ratio when $C_{h_\alpha} = 0$. The undamped natural frequency of the airframe and control modes when $C_{h_\alpha} = 0$ is readily approximated by the following expressions:

$$\omega_{n_a}^2 = -\frac{C_{m_\alpha}}{I_Y/qS\bar{c}} \tag{5}$$

$$\omega_{n_c}^2 = -\frac{C_{h_\delta}}{I_c/qS_c\bar{c}_c} \tag{6}$$

The value of the ratio for peak airframe damping then becomes

$$\frac{\omega_{n_c}}{\omega_{n_a}} = K = \sqrt{\frac{C_{n_\delta}\dfrac{I_Y}{S\bar{c}}}{C_{m_\alpha}\dfrac{I_c}{S_c\bar{c}_c}}} \tag{7}$$

This expression for the value of the ratio when $C_{h_\alpha} = 0$ is seen to be independent of altitude if the value of C_{h_δ} is dependent upon aerodynamic forces only and is not the sum of an aerodynamic force and a spring force as discussed in the section of the paper entitled "General Comments on the Application of Floating Controls."

Determination of ω_{n_a} for Specified Conditions of C_{h_α} and C_{h_δ}

Writing the fourth-order characteristic equation as follows:

$$p^4 + \frac{B}{A} p^3 + \frac{C}{A} p^2 + \frac{D}{A} p + \frac{E}{A} = 0 \tag{8}$$

and assuming that it can be factored into two quadratic factors representing the airframe and control modes of motion results in the following characteristic-equation representation:

$$\left(p^2 + 2\zeta_a\omega_{n_a} p + \omega_{n_a}{}^2\right)\left(p^2 + 2\zeta_c\omega_{n_c} p + \omega_{n_c}{}^2\right) = 0 \tag{9}$$

By inspection, the value of the coefficient E/A is $\omega_{n_a}{}^2\omega_{n_c}{}^2$ and if $\omega_{n_c}{}'/\omega_{n_a}{}' = K$, then for peak airframe damping

$$\frac{E}{A} = K^2\left(\omega_{n_a}{}'\right)^4 \tag{10}$$

Referring to the coefficients of the characteristic equation as previously defined for equation (4) of the text and obtaining an approximate evaluation for E/A by selecting the most important parameters yields

$$\frac{E}{A} = \frac{a_1 b_3 C_{h_\delta} - a_1 b_5 C_{h_\alpha}}{a_1 b_1 c_1} \tag{11}$$

Equating equations (10) and (11) gives the expression

$$\frac{E}{A} = \frac{a_1 b_3 C_{h_\delta} - a_1 b_5 C_{h_\alpha}}{a_1 b_1 c_1} = K^2\left(\omega_{n_a}{}'\right)^4 \tag{12}$$

from which the undamped natural frequency of the airframe at peak airframe damping can be obtained for any specified values of C_{h_α} and C_{h_δ} and any flight condition. Once ω_{n_a}' is determined from equation (12), the undamped natural frequency of the control mode is easily computed from equation (7).

Determination of the Value of ζ_c' for Peak Airframe Damping

The constant value of ζ_c' for peak airframe damping as shown in figures 9 and 11(b) can be estimated if it is assumed that for peak airframe damping the control motion lags the airframe motion by 45° and the frequency at which the control motion lags the airframe motion by 45° is the undamped natural frequency of the airframe, which for this case is ω_{n_a}'. Although the frequency of the disturbed airframe oscillation will not be the undamped airframe natural frequency, the error induced by this assumption is negligible. This can be verified by plotting the frequency response of the airframe and control modes of motion for a combination of control parameters that gives peak airframe damping. The frequency response plot shows that at frequencies near the airframe undamped natural frequency the phase angle of the control mode is relatively insensitive to small changes in frequency. Therefore, only slight changes in the phase-angle magnitude will result if the disturbed airframe frequency is different from the undamped natural frequency of the airframe.

The phase angle ϕ of a quadratic factor of the general form

$$\left(p^2 + 2\zeta\omega_n p + \omega_n^2\right) \tag{13}$$

at a particular frequency (ω) is defined by the following expression (ref. 6):

$$\phi = -\tan^{-1} \frac{2\zeta\left(\frac{\omega}{\omega_n}\right)}{1 - \left(\frac{\omega}{\omega_n}\right)^2} \tag{14}$$

For this case, let equation (13) take the form of the control mode

$$\left(p^2 + 2\zeta_c\omega_{n_c} p + \omega_{n_c}^2\right)$$

and in equation (14), let the phase angle $\phi = \phi_c = 45^\circ$, let the frequency ω be the natural frequency of the airframe ω_{n_a}' let $\omega_n = \omega_{n_c}'$, and let $\zeta = \zeta_c'$. With these substitutions, equation (14) can be rewritten in terms of the control-mode parameters as follows:

$$\phi_c = 45^\circ = -\tan^{-1} \frac{2\zeta_c' \left(\frac{\omega_{n_a}'}{\omega_{n_c}'}\right)}{1 - \left(\frac{\omega_{n_a}'}{\omega_{n_c}'}\right)^2} \tag{15}$$

Solving equation (15) for ζ_c' gives

$$\zeta_c' = \frac{1 - \left(\frac{\omega_{n_a}'}{\omega_{n_c}'}\right)^2}{2\left(\frac{\omega_{n_a}'}{\omega_{n_c}'}\right)} \tag{16}$$

and, if $\left(\omega_{n_c}'/\omega_{n_a}'\right) = K$ as before, yields

$$\zeta_c' = \frac{K^2 - 1}{2K} \tag{17}$$

Determination of $C_{h_{\dot{\delta}}}'$ for Peak Airframe Damping

Equation (17) gives the value of the control-mode damping ζ_c' that gives peak airframe damping. Once this value of ζ_c' has been determined for a particular flight condition the control-surface damping rate governed by the value of $C_{h_{\dot{\delta}}}'$ can be readily determined from the following relation:

$$2\zeta_c'\omega_{n_c}' = \frac{C_{h_{\dot{\delta}}}'}{I_c/qS_c\bar{c}_c} \tag{18}$$

Determination of the Peak Airframe Damping ζ_a'

Up to this point it has been possible to choose a flight condition, select the values of C_{h_α} and C_{h_δ}, and then to predict the control dynamic characteristics, the control damping rate, and the airframe undamped natural frequency that gives a peak value of airframe damping ζ_a'. The value of ζ_a' can be approximated by proceeding along the following lines. Rewriting equation (9) in terms of the already known quantities gives

$$\left[p^2 + 2\zeta_a'\omega_{n_a}'p + \left(\omega_{n_a}'\right)^2\right]\left[p^2 + 2\left(\frac{K^2 - 1}{2K}\right)\left(K\omega_{n_a}'\right)p + K^2\left(\omega_{n_a}'\right)^2\right] \quad (19)$$

Now writing equation (19) in the form of equation (8) and equating coefficients of like powers to the coefficients of equation (8) gives for the value of C/A

$$\frac{C}{A} = \left(\omega_{n_a}'\right)^2\left[1 + 2\zeta_a'\left(K^2 - 1\right) + K^2\right] \quad (20)$$

Referring again to the definition of the coefficients of equation (4) as previously defined in the text, an approximate evaluation for C/A can be obtained by selecting the most important parameters. Thus,

$$\frac{C}{A} = \frac{a_1b_2C_{h_{\dot\delta}}' - a_2b_1C_{h_{\dot\delta}}' - a_1b_1C_{h_\delta} - a_1b_3c_1}{a_1b_1c_1} \quad (21)$$

Equating equations (20) and (21) gives the following expression in which all quantities are known except ζ_a':

$$-\frac{C_{h_{\dot\delta}}'}{c_1}\left(\frac{a_2}{a_1} - \frac{b_2}{b_1}\right) - \left(\frac{b_3}{b_1} + \frac{C_{h_\delta}}{c_1}\right) = \left(\omega_{n_a}'\right)^2\left[1 + 2\zeta_a'\left(K^2 - 1\right) + K^2\right] \quad (22)$$

Sample Calculation

The procedure that has been outlined could probably be more clearly understood if a sample calculation were made. The airframe is the airframe of this analysis and the floating controls are assumed aft of the center of gravity. The flight condition to be investigated is M = 2.0 at sea level and the values of the floating-control hinge-moment coefficients are $C_{h_\alpha} = -0.8$ and $C_{h_\delta} = -0.2$. The problem is to determine the

viscous damping rate that will give maximum airframe damping for the assumed conditions and the value of the airframe damping ζ_a'.

I - Determination of the value of the ratio $\omega_{n_c}/\omega_{n_a} = K$ as shown in figure 10:

$$\left(\omega_{n_a}^2\right)_{C_{h_\alpha}=0} = -\frac{C_{m_\alpha}}{I_Y/qS\bar{c}} = -\frac{(-1.27)}{7.188 \times 10^{-4}} = 1,767$$

$$\left(\omega_{n_c}^2\right)_{C_{h_\alpha}=0} = -\frac{C_{h_\delta}}{I_c/qS_c\bar{c}_c} = -\frac{(-0.2)}{3.165 \times 10^{-6}} = 63,191$$

$$\left(\frac{\omega_{n_c}'}{\omega_{n_a}'}\right)^2 = K^2 = \frac{63191}{1767} = 35.765$$

$$K = 5.98$$

II - Determination of the value of E/A for C_{h_α} and C_{h_δ} selected:

$$\frac{E}{A} = \frac{a_1b_3C_{h_\delta} - a_1b_5C_{h_\alpha}}{a_1b_1c_1}$$

$$\frac{E}{A} = \frac{(0.4624)(-1.27)(-0.2) - (0.4624)(-0.206)(-0.8)}{10.522 \times 10^{-10}}$$

$$\frac{E}{A} = 39.20 \times 10^6$$

III - Determination of the peak airframe natural frequency and control natural frequency for C_{h_α} and C_{h_δ} selected:

$$K^2\left(\omega_{n_a}'\right)^4 = E/A = 39.20 \times 10^6$$

$$\left(\omega_{n_a}'\right)^4 = \frac{39.20 \times 10^6}{35.765} = 1.096 \times 10^6$$

$$\omega_{n_a}' = 32.36$$

$$\omega_{n_c}' = K\omega_{n_a}' = (5.98)(32.36)$$

$$\omega_{n_c}' = 193.5$$

IV - Determination of the constant value of ζ_c' as shown in figure 9:

$$\zeta_c' = \frac{K^2 - 1}{2K} = \frac{35.765 - 1}{2(5.98)}$$

$$\zeta_c' = 2.91$$

V - Determination of magnitude of control-surface damping coefficient $C_{h_{\dot\delta}}'$:

$$-\frac{C_{h_{\dot\delta}}'}{I_c/qS_c\bar{c}_c} = 2\zeta_c'\omega_{n_c}'$$

$$-\frac{C_{h_{\dot\delta}}'}{3.165 \times 10^{-6}} = 2(2.91)(193.5)$$

$$C_{h_{\dot\delta}}' = -0.00356$$

or the required viscous damping rate is

$$H_{\dot\delta} = -2.74 \text{ ft-lb/radian/sec}$$

CONFIDENTIAL

VI - Determination of magnitude of airframe damping parameter ζ_a':

$$-\frac{C_{h_{\dot{\delta}}}'}{c_1}\left(\frac{a_2}{a_1}-\frac{b_2}{b_1}\right)-\left(\frac{b_3}{b_1}+\frac{C_{h_\delta}}{c_1}\right)=\left(\omega_{n_a}'\right)^2\left[1+2\zeta_a'\left(K^2-1\right)+K^2\right]$$

$$-\frac{(-3.56\times10^{-3})}{3.165\times10^{-6}}\left[\frac{2.46}{0.4624}-\frac{(-2.94\times10^{-3})}{7.188\times10^{-4}}\right]-\left[\frac{(-1.27)}{7.188\times10^{-4}}+\frac{(-0.2)}{3.165\times10^{-6}}\right]=$$

$$(32.36)^2\left[1+2(\zeta_a')(35.765-1)+(35.765)\right]$$

or

$$10{,}585+64{,}958=38{,}491+72{,}792\zeta_a'$$

$$\zeta_a'=0.51$$

REFERENCES

1. Greenberg, Harry, and Sternfield, Leonard: A Theoretical Investigation of Longitudinal Stability of Airplanes With Free Controls Including Effect of Friction in Control System. NACA Rep. 791, 1944. (Supersedes NACA ARR 4B01.)

2. Crane, Harold L., Hurt, George J., Jr., and Elliott, John M.: Subsonic Flight Investigation of Methods To Improve the Damping of Lateral Oscillations by Means of a Viscous Damper in the Rudder System in Conjunction With Adjusted Hinge-Moment Parameters. NACA RM L54D09, 1954.

3. Seaberg, Ernest C., and Smith, Earl F.: Theoretical Investigation of an Automatic Control System With Primary Sensitivity to Normal Accelerations As Used To Control a Supersonic Canard Missile Configuration. NACA RM L51D23, 1951.

4. Anon.: Methods of Analysis and Synthesis of Piloted Aircraft Flight Control Systems. Vol. 1. Rep. No. AE-61-4, Bur. Aero., Oct., 1952.

5. Sternfield, Leonard, and Gates, Ordway B., Jr.: A Method of Calculating a Stability Boundary That Defines a Region of Satisfactory Period-Damping Relationship of the Oscillatory Mode of Motion. NACA TN 1859, 1949.

6. Brown, Gordon S., and Campbell, Donald P.: Principles of Servomechanisms. John Wiley & Sons, Inc., 1948.

TABLE I

ESTIMATED LONGITUDINAL STABILITY DERIVATIVES

[Static margin of 0.56$\bar{c}$ at M = 1.6]

Mach number	q, lb/sec	V, ft/sec	C_{m_q}	C_{m_α}	$C_{m_{\dot{\alpha}}}$	C_{L_α}	C_{m_δ} (canards)	C_{m_δ} (wing tip)	C_{L_δ} (wing tip)[1]
1.2	2,132	1,339	-8.88	-1.83	-0.987	3.02	0.820	-0.328	0.15
1.6	3,791	1,785	-8.47	-1.47	-.941	2.61	.702	-.244	.132
2.0	5,980	2,245	-7.43	-1.27	-.826	2.46	.573	-.206	.114
1.2 (15,000 ft)	1,200	1,269	-----	-----	-----	----	-----	-----	-----

[1] C_{L_δ} assumed zero for canards.

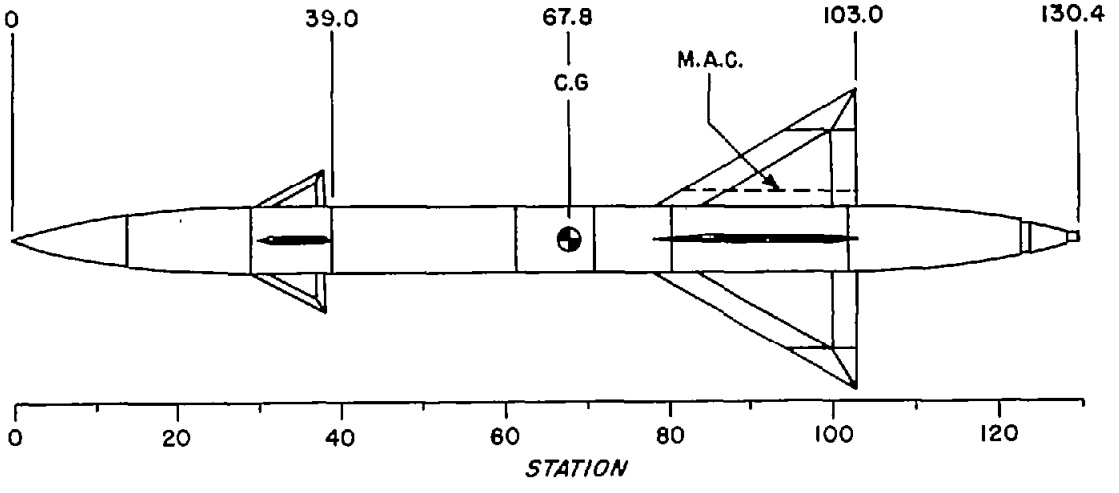

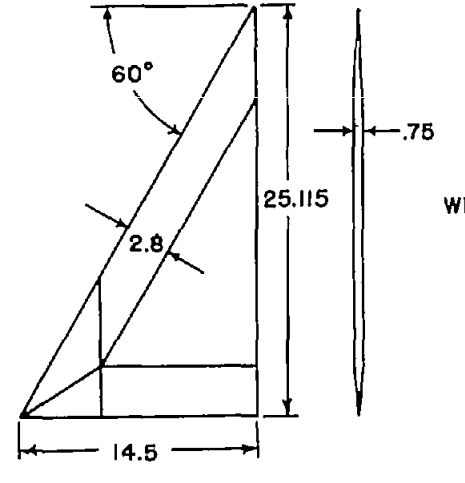

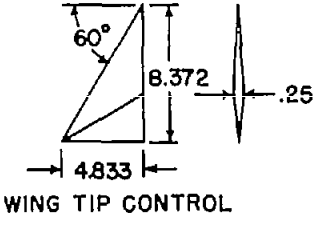

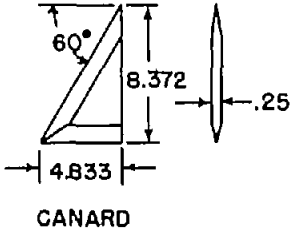

MODEL WEIGHT, LB	162.5
MOMENT OF INERTIA, SLUG-FT^2	31.3
BODY LENGTH, INCHES	130.4
BODY DIAMETER, INCHES	8.0
WING SPAN, INCHES	37.0
TOTAL WING AREA ONE PLANE, FT^2	4.1
CANARD-FIN SPAN, INCHES	17.7
EXPOSED CANARD AREA, ONE PLANE, FT^2	0.281
WING M.A.C., FT	1.776
CANARD M.A.C., FT	.458

Figure 1.- Sketch of airframe configuration. (All dimensions in inches unless otherwise noted.)

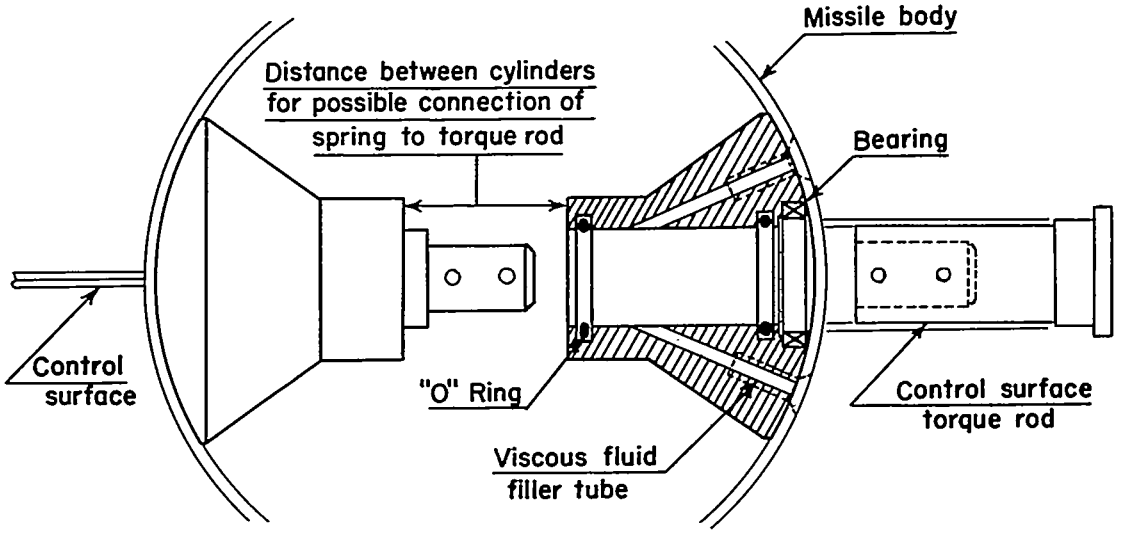

NOTE: Gap distance between control surface torque rod and inner surface of cylinder depends upon viscosity of fluid and damping rate desired.

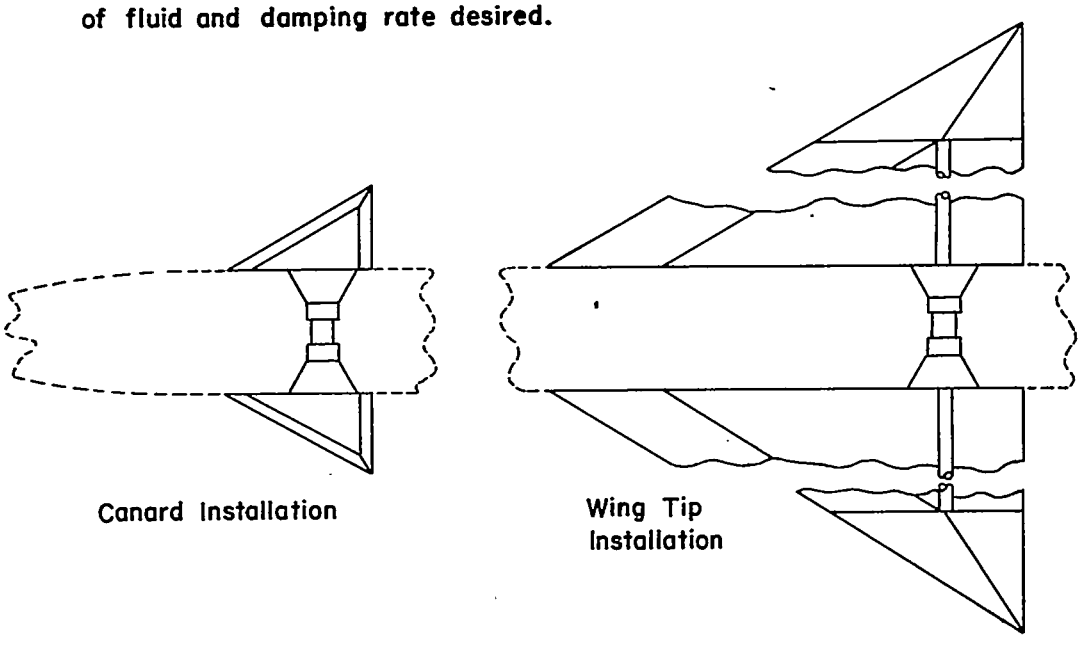

Figure 2.- Sketch of proposed viscous damper for use with floating control surfaces with two typical installations shown.

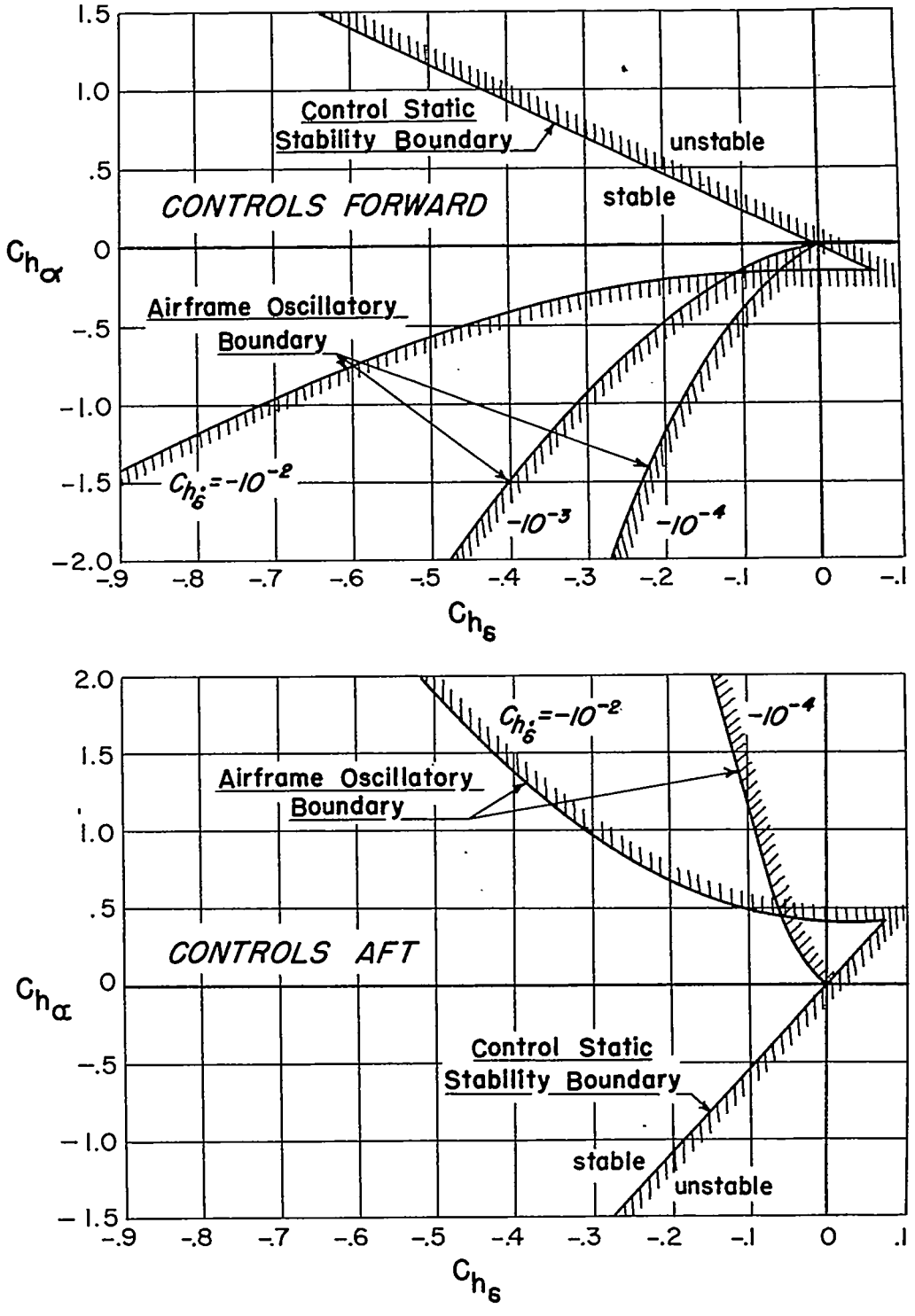

Figure 3.- Stability boundaries for the airframe with floating controls aft and forward of the airframe center of gravity. M = 1.2 at sea level.

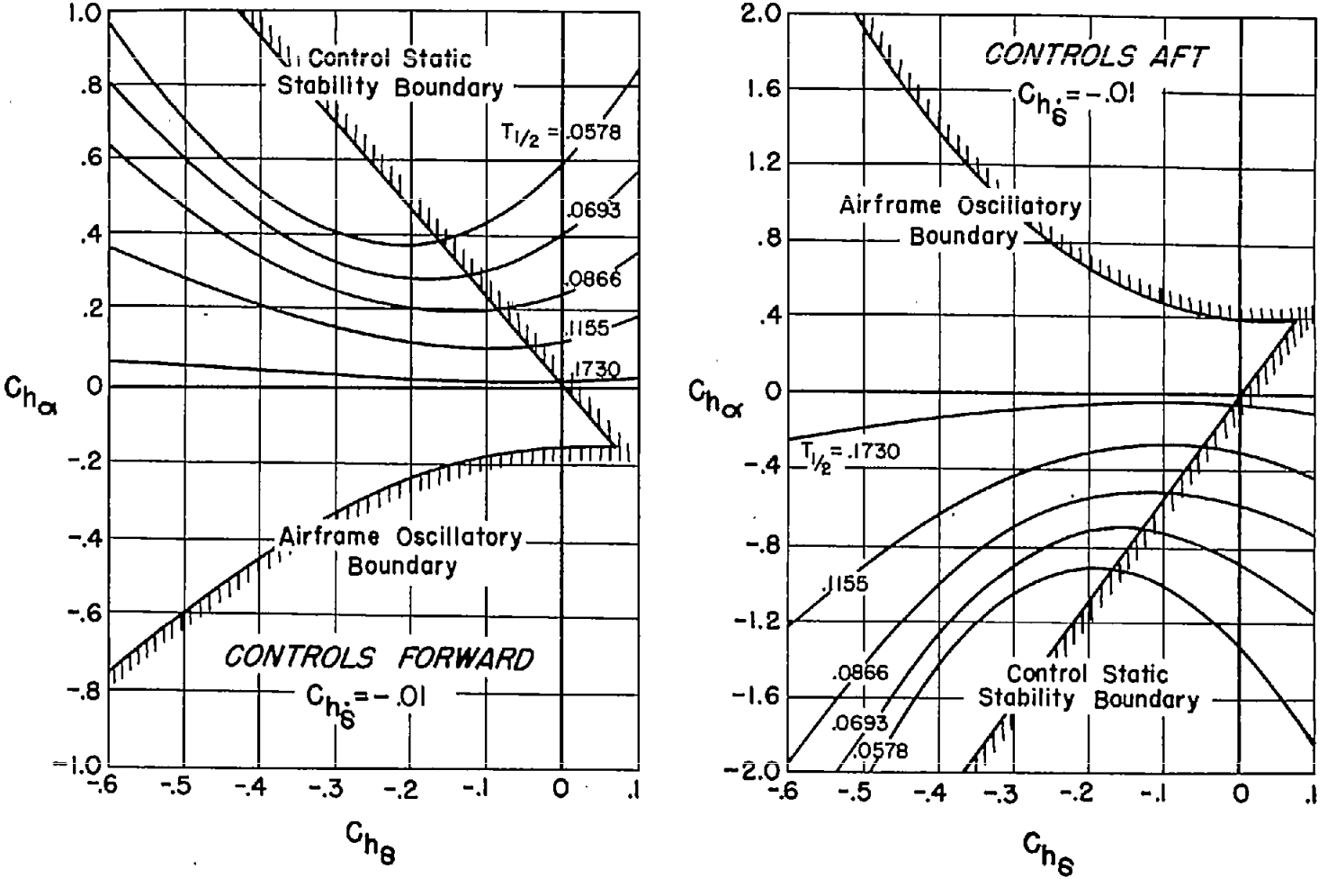

Figure 4.- Effect of varying C_{h_α} and C_{h_δ} on airframe time to damp to half amplitude for floating controls aft or forward of the airframe center of gravity. $C_{h_{\dot{\delta}}} = -0.01$; M = 1.2 at sea level.

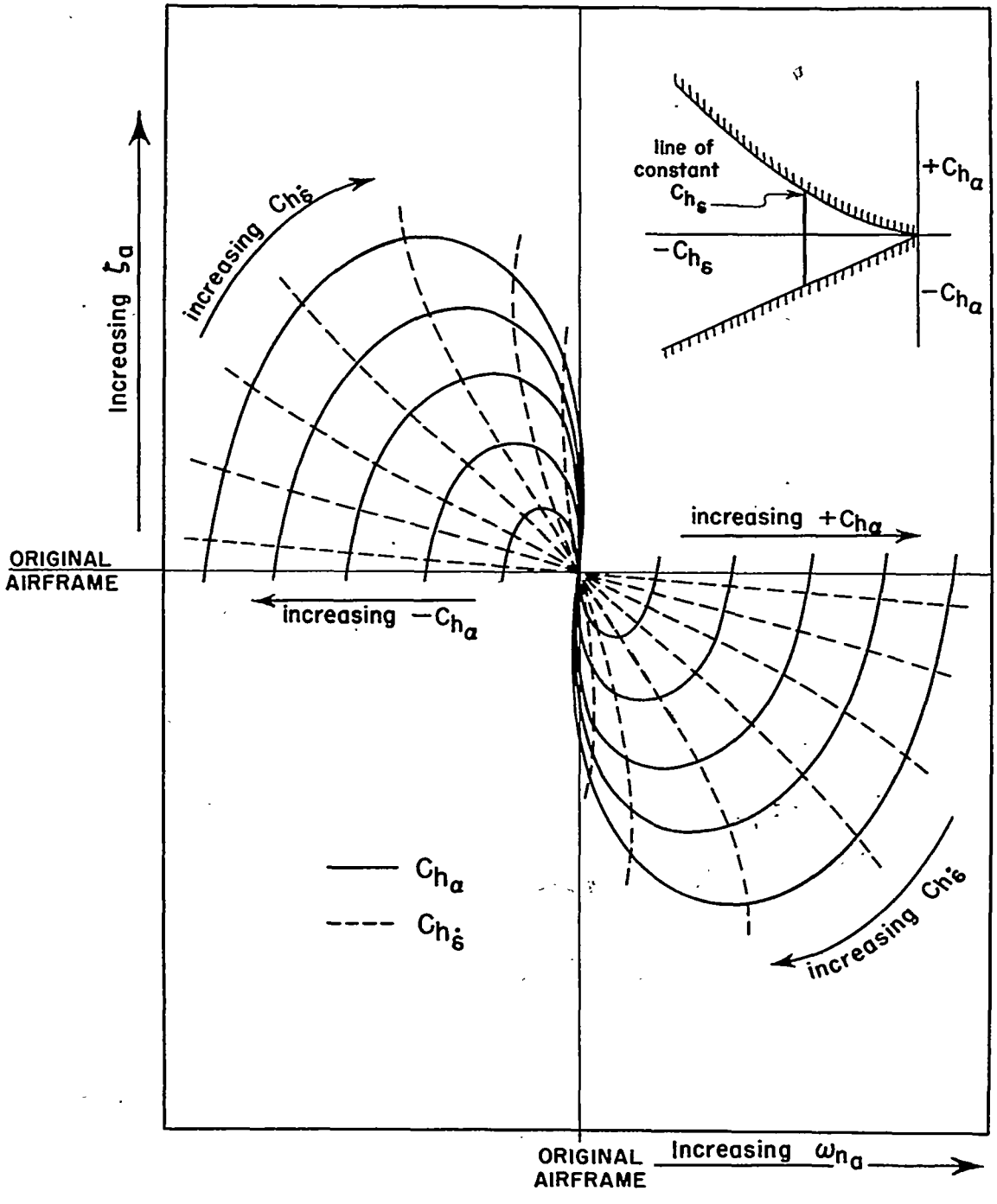

Figure 5.- Typical variation of airframe damping and natural frequency along a line of constant C_{h_δ} in the stable region. (Increasing ζ_a and ω_{n_a} in direction as indicated by arrows.)

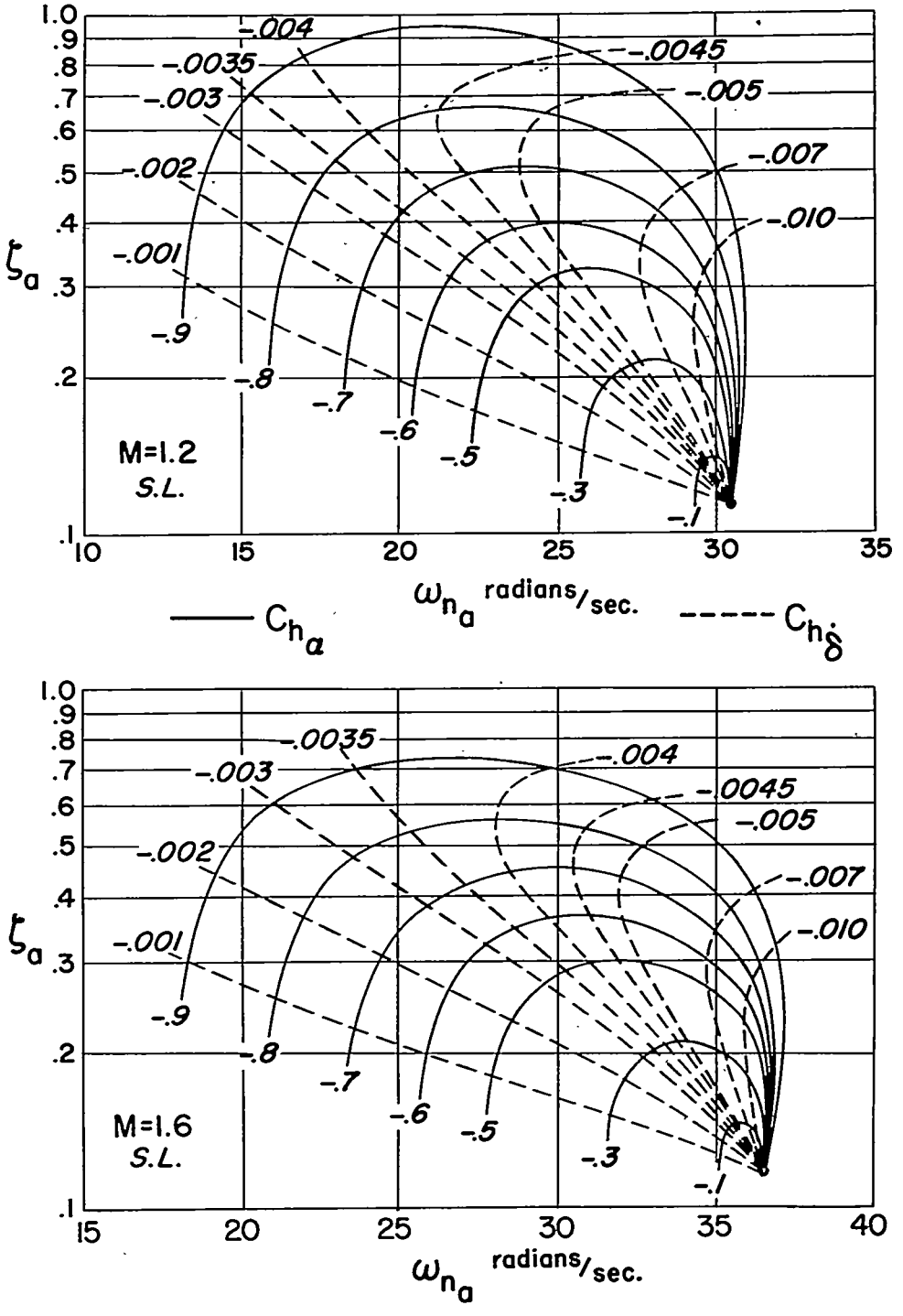

(a) M = 1.2 and 1.6 at sea level.

Figure 6.- Effect on airframe damping and natural frequency of varying C_{h_α} and $C_{h_{\dot{\delta}}}$. Floating controls aft; C_{h_δ} = -0.2.

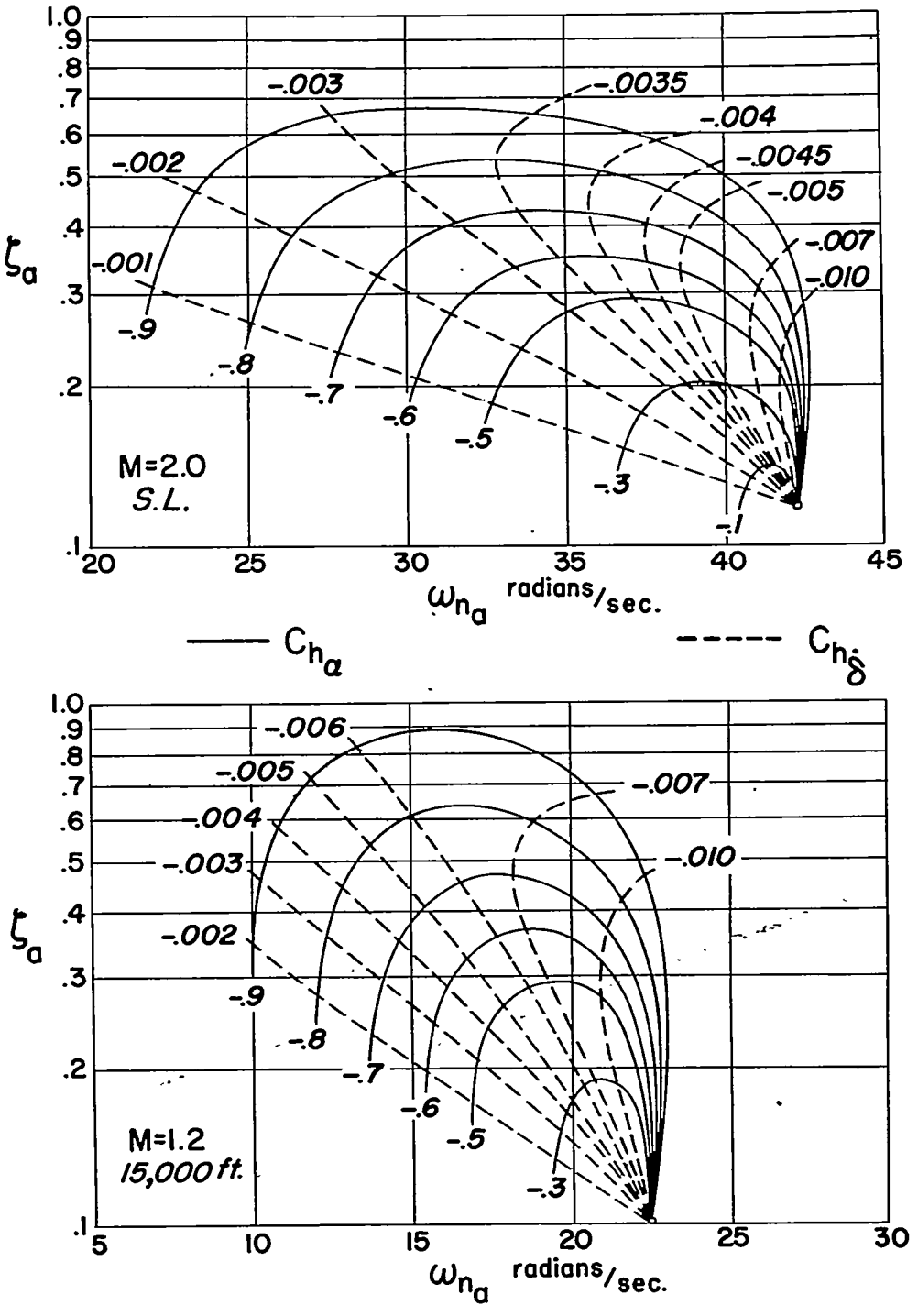

(b) M = 2.0 at sea level and M = 1.2 at 15,000 feet.

Figure 6.- Concluded.

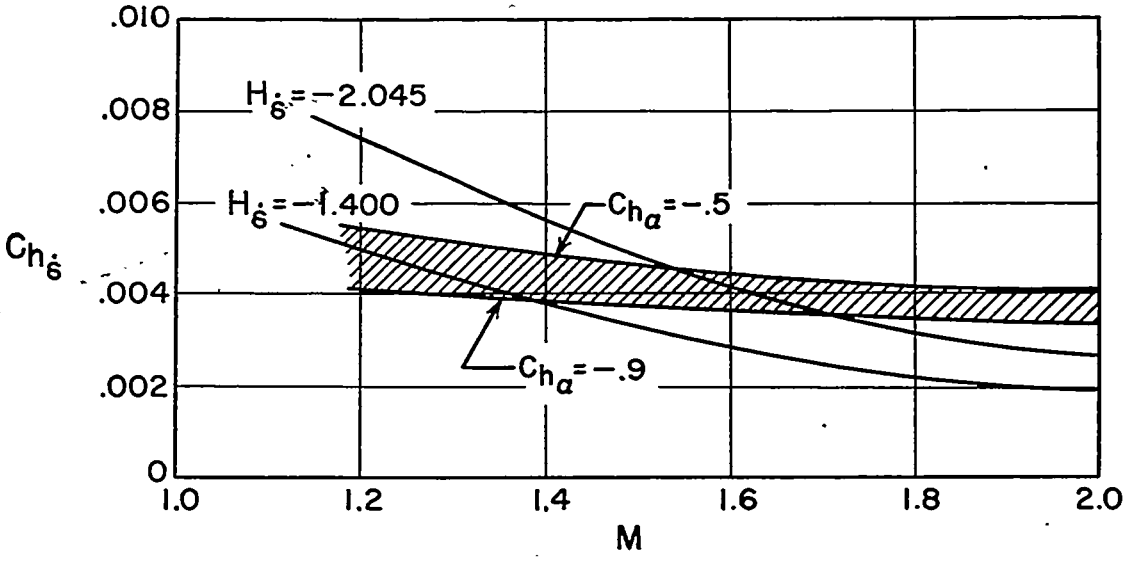

Figure 7.- Variation of $C_{h_{\dot{\delta}}}$ with Mach number for two constant values of $H_{\dot{\delta}}$ compared with the desired variation shown as the shaded area. Floating controls aft; C_{h_δ} = -0.2.

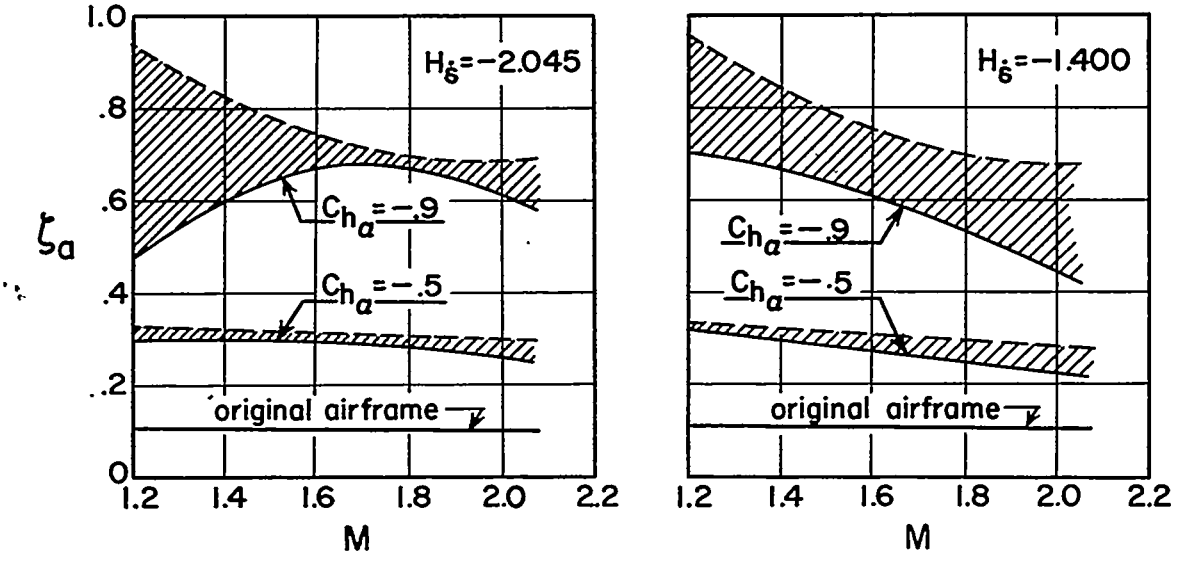

Figure 8.- Variation of floating-control airframe damping with Mach number for two values of $H_{\dot{\delta}}$ shown by solid curve for two values of C_{h_α} and compared with maximum possible airframe damping represented by dashed curve. Floating controls aft; C_{h_δ} = -0.2 at sea level.

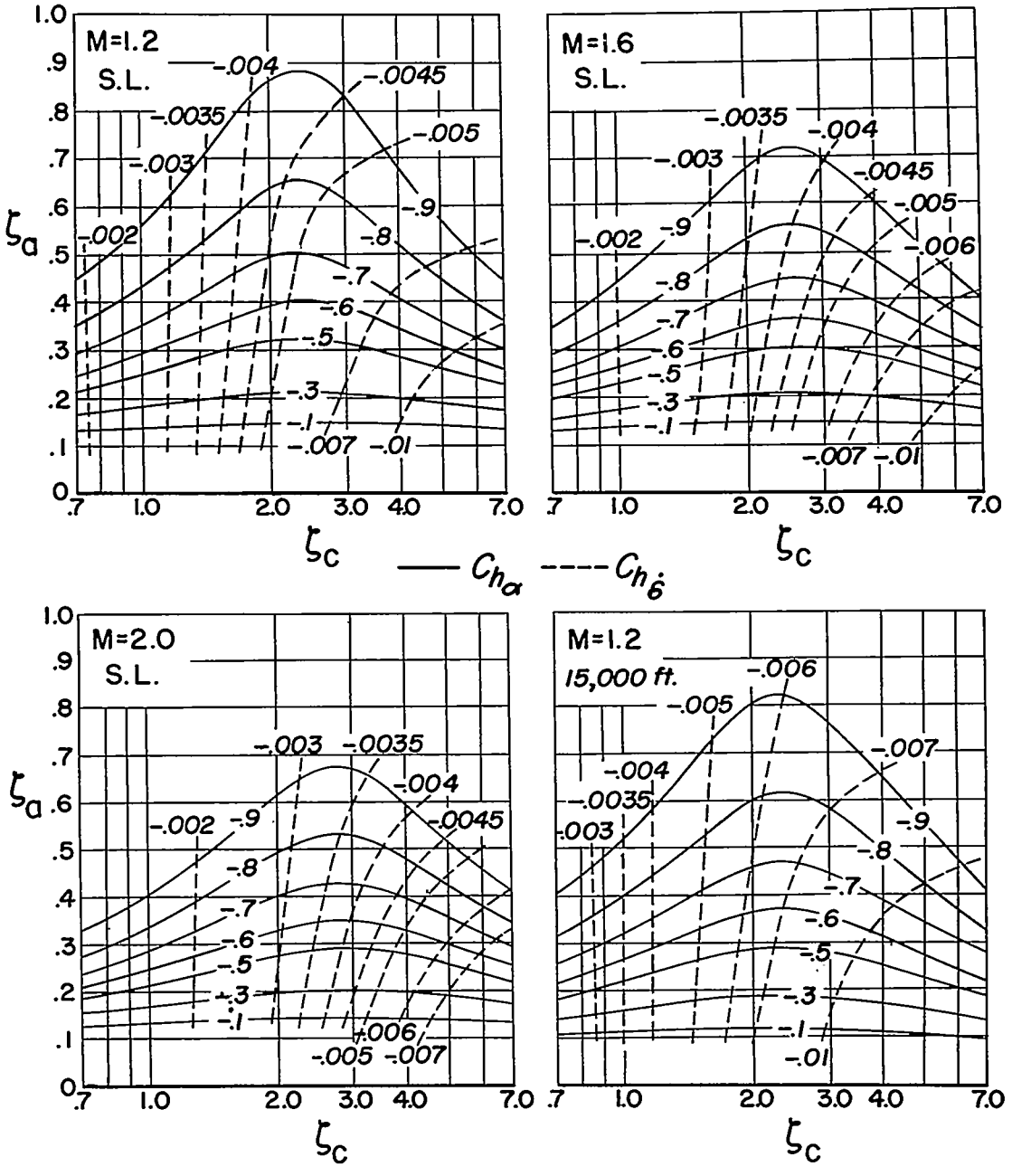

Figure 9.- Variation of airframe damping parameter ζ_a with the floating-control damping parameter ζ_c for various values of C_{h_α} and $C_{h_{\dot\delta}}$. Floating controls aft; C_{h_δ} = -0.2.

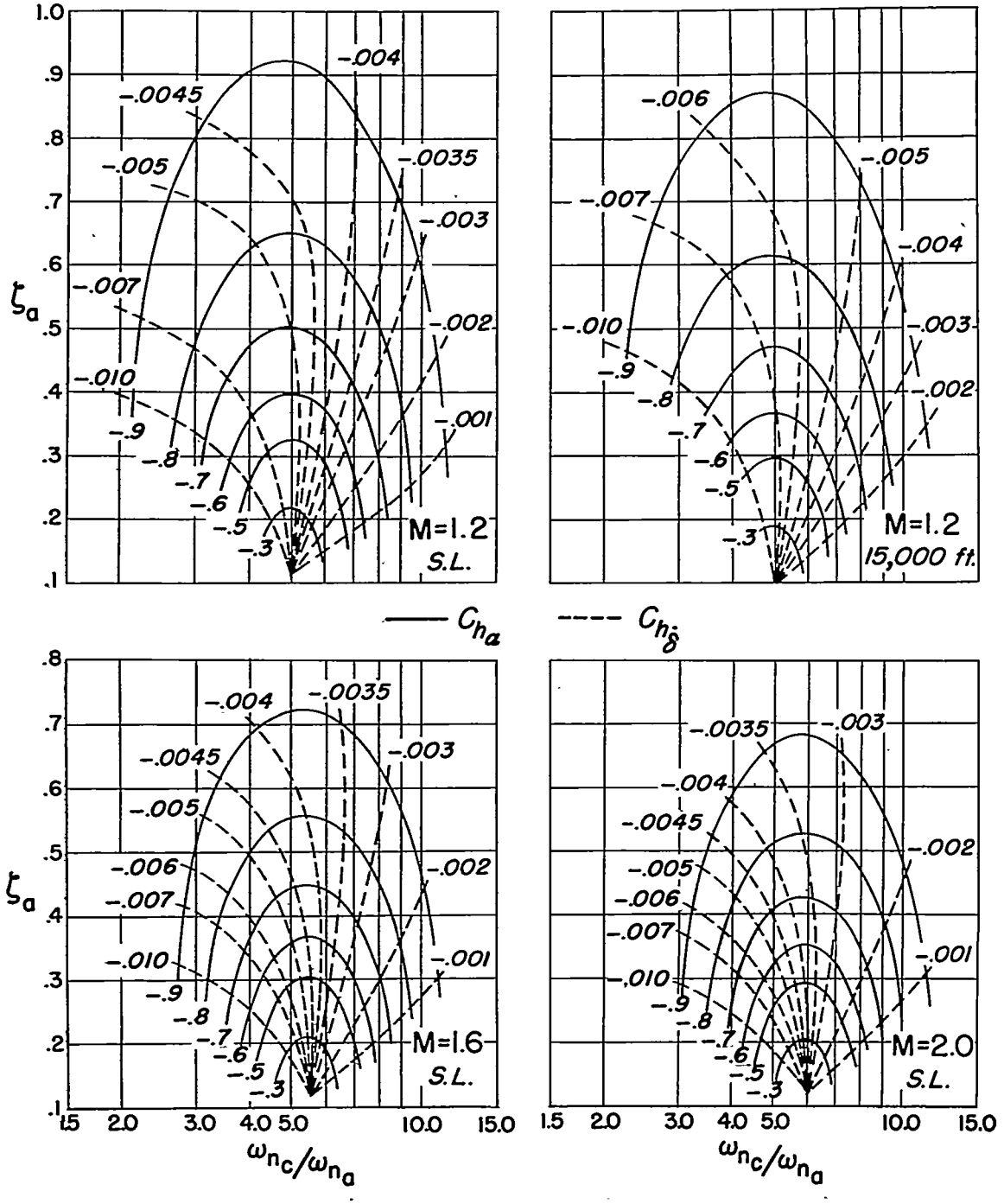

Figure 10.- Variation of airframe damping parameter ζ_a with the ratio of the floating-control undamped natural frequency to the airframe undamped natural frequency for various values of C_{h_α} and $C_{h_{\dot{\delta}}}$. Floating controls aft; C_{h_δ} = -0.2.

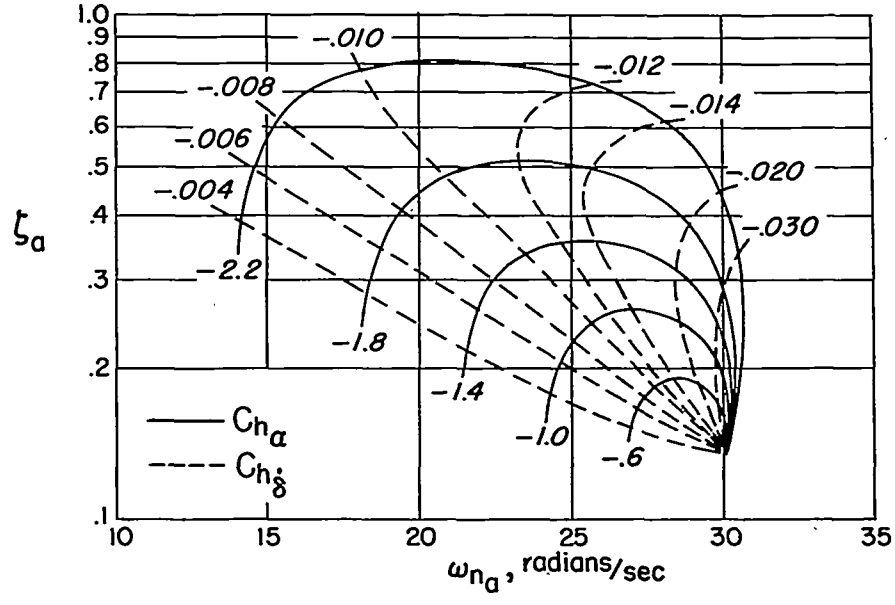

(a) Effect on airframe damping ζ_a and natural frequency ω_{n_a} of varying C_{h_α} and $C_{h_{\dot\delta}}$.

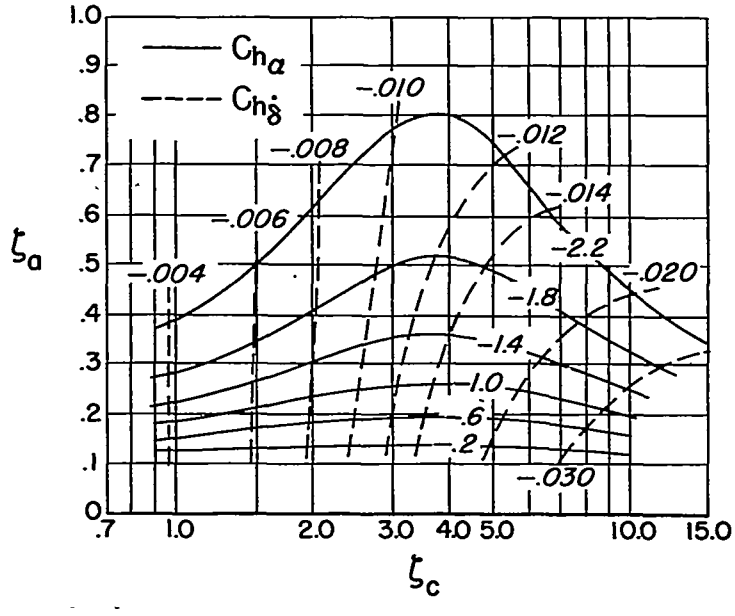

(b) Variation of airframe damping ζ_a with floating-control damping ζ_c for various values of C_{h_α} and $C_{h_{\dot\delta}}$.

Figure 11.- Airframe and control dynamic characteristics for $C_{h_\delta} = -0.5$. Floating controls aft; M = 1.2 at sea level.

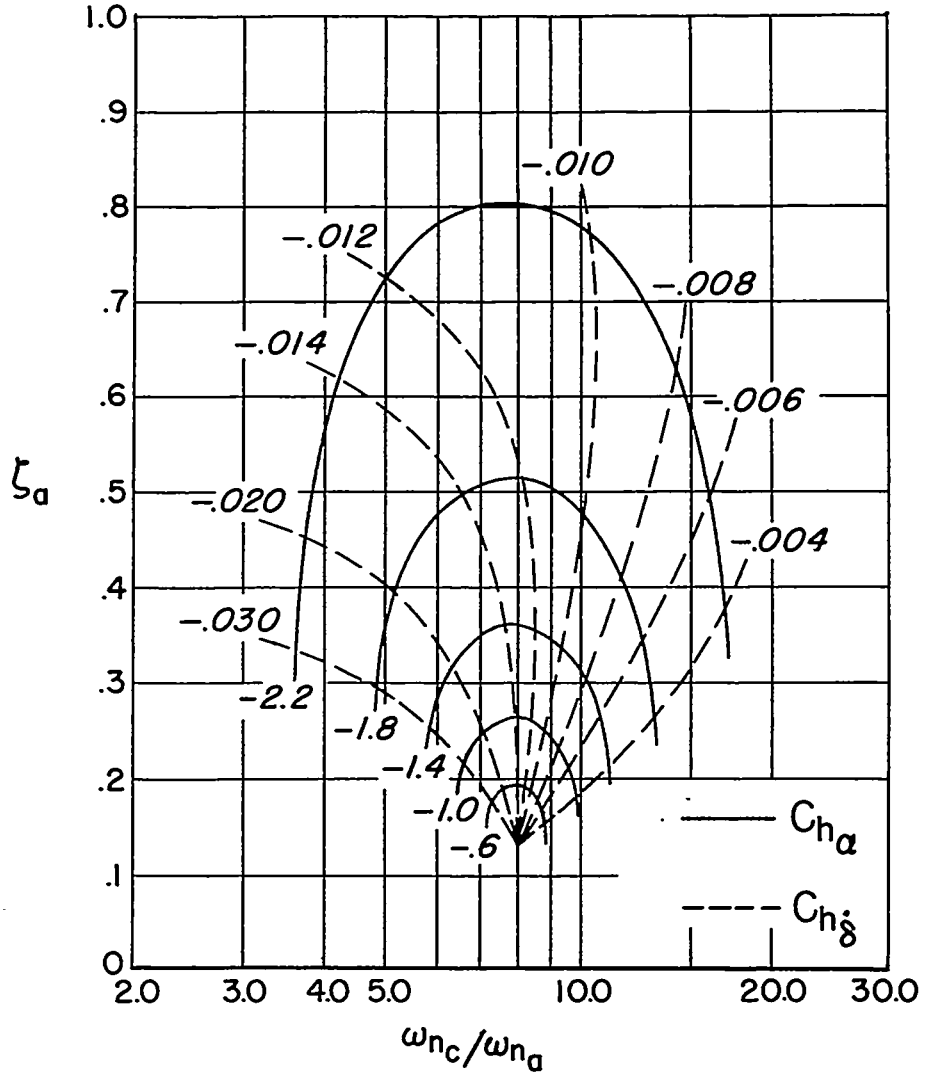

(c) Variation of airframe damping ζ_a with the ratio of the floating-control undamped natural frequency to the airframe undamped natural frequency for various values of C_{h_α} and $C_{h_{\dot{\delta}}}$.

Figure 11.- Concluded.